Construction of Nanostructured Carbonaceous Films by the Layer-by-Layer Self-Assembly of Poly(diallyldimethylammonium) Chloride and Poly(amic acid) and Subsequent Pyrolysis

Isamu Moriguchi,[†] Yasutake Teraoka,[†] Shuichi Kagawa,[†] and Janos H. Fendler*[,‡]

Department of Applied Chemistry, Faculty of Engineering, Nagasaki University, 1-14 Bunkyo-machi, Nagasaki 852-8521, Japan, and Center for Advanced Material Processing, Clarkson University, P.O. Box 5814, Potsdam, New York 13699

Received January 25, 1999. Revised Manuscript Received April 14, 1999

Poly(diallyldimethylammonium chloride), **PD**, and poly(amic acid), **PA**, were layer-by-layer self-assembled onto quartz and mica substrates, S. Quantitative formation of the self-assembled films, S−(**PD**/**PA**)$_n$, were characterized by absorption spectroscopy, by quartz crystal microbalance measurements, and by scanning force microscopy (AFM). Pyrolysis of the S−(**PD**/**PA**)$_n$ films by heating to 1000 °C proceeded via the formation of subsequent carbonization of a polyimide intermediate which ultimately produced a graphite-like carbonaceous film with conductivities in the 150−200 S cm^{-1} range. AFM images indicated the assembly of laminar carbon nano islands with increasing n in S−(**PD**/**PA**)$_n$.

Introduction

Graphite-like carbonaceous materials are fruitfully employed as electrodes in high charge density lithium batteries. They are usually prepared by the pyrolysis of organic polymers.[1−7] The importance of the chemical structure of precursor polymers has been realized.[8−10] Attempts to control the structure and properties of the carbonaceous films were made by the pyrolysis of polymers organized in Langmuir−Blodgett (LB) films[11] and in the cavities of mesoporous silica[12] and zeolites.[13] For example, the pyrolysis of the LB films resulted in the formation of graphite-like ultrathin film with high conductivity even at a relatively low temperature.[11]

Self-assembly has been shown to provide a convenient and versatile method for the formation of ultrathin films. The method is deceptively simple. It involves the sequential adsorption of nanometer-thick layers of oppositely charged polyelectrolytes,[13−18] polyelectrolytes and inorganic nanoparticles,[19−26] and polyelectrolytes and graphite oxides.[27−30] The major attraction of self-assembly is that any number of layers of polyelectrolytes of any composition can be adsorbed onto a large variety of structurally different substrates in any desired order. In a recent study, electrodes prepared by the layer-by-layer assembly of colloidal graphite oxide nanoplatelets and nanolayers of poly(diallyldimethylammonium) chloride and polyoxyethylene have been shown to function as a high charge density lithium ion intercalation battery.[29]

The present study describes the construction and characterization of an ultrathin carbonaceous film by the layer-by-layer self-assembly of poly(diallyldimethylammonium chloride) and poly(amic acid) and subsequent pyrolysis. Our choice of polyelectrolytes was dictated by the demonstrated satisfactory self-assembly of these materials.

[†] Nagasaki University.
[‡] Clarkson University.

(1) Brom, H. B.; Tomkiewicz, Y.; Aviram, A.; Broers, A.; Sunners, B. *Solid State Commun.* **1980**, *35*, 435.
(2) Moore, A. W. *Chemistry and physics of carbon*; Walker, P. L., Jr., Thrower, P. A., Eds.; Marcel Dekker: New York, 1973; Vol. 11, p 697.
(3) Kittlesen, G. P.; White, H. S.; Wrighton, M. S. *J. Am. Chem. Soc.* **1984**, *106*, 5375.
(4) Hu, C. Z.; Andrade, J. D. *J. Appl. Polym. Sci.* **1985**, *30*, 4409.
(5) Chiang, L. Y. *J. Chem. Soc., Chem. Commun.* **1987**, 304.
(6) Ohnishi, T.; Murase, I.; Noguchi, T.; Horooka, M. *Synth. Met.* **1987**, *18*, 497.
(7) Hishiyama, Y.; Yoshida, A.; Inagaki, M. *Carbon* **1998**, *36*, 1113.
(8) Murakami, M.; Yoshimura, S. *Synth. Met.* **1987**, *18*, 509.
(9) Zheng, T.; Liu, Y.; Fuller, E. W.; Tseng, S.; Sacken, U.; Dahn, J. R. *J. Electrochem. Soc.* **1995**, *142*, 2581.
(10) Suh, M. C.; Shim, S. C. *Chem. Mater.* **1997**, *9*, 192.
(11) Akatsuka, T.; Tanaka, H.; Toyama, J.; Nakamura, T.; Kawabata, Y. *Chem. Lett.* **1990**, 975.
(12) Wu, C. G.; Bein, T. *Science* **1994**, *266*, 1013.
(13) Johnson, S. A.; Sringham, E. S.; Olliver, R. J.; Mallouk, T. E. *Chem. Mater.* **1997**, *9*, 2448.
(14) Decher, G.; Schmitt, J. *Prog. Colloid Polym. Sci.* **1992**, *89*, 160.
(15) Lvov, Y.; Haas, H.; Decher, G.; Mohwald, H.; Kalachev, A. *J. Phys. Chem.* **1993**, *97*, 12835.
(16) Lvov, Y.; Essler, F.; Decher, G. *J. Phys. Chem.* **1993**, *97*, 13773.
(17) Fou, A. C.; Rubner, M. F. *Macromolecules* **1995**, *28*, 7115.
(18) Fendler, J. H. *Chem. Mater.* **1996**, *8*, 1616.
(19) Keller, S. W.; Kim, H. N.; Mallouk, T. E. *J. Am. Chem. Soc.* **1994**, *116*, 8817.
(20) Kleinfeld, E. R.; Ferguson, G. S. *Science* **1994**, *265*, 370.
(21) Fendler, J. H.; Meldrum, F. C. *Adv. Mater.* **1995**, *7*, 607.
(22) Kotov, N. A.; Dekany, I.; Fendler, J. H. *J. Phys. Chem.* **1995**, *99*, 13065.
(23) Freeman, R. G.; Grabar, K. C.; Allison, K. J.; Bright, R. M.; Davis, J. A.; Guthrie, A. P.; Hommer, M. B.; Jackson, M. A.; Smith, P. C.; Walter, D. G.; Natan, M. J. *Science* **1995**, *267*, 1629.
(24) Kleinfeld, E. R.; Ferguson, G. S. *Chem. Mater.* **1996**, *8*, 1575.
(25) Schmitt, J.; Decher, G. *Adv. Mater.* **1997**, *9*, 61.
(26) Moriguchi, I.; Fendler, J. H. *Chem. Mater.* **1998**, *10*, 2205.
(27) Kotov, N. A.; Dekany, I.; Fendler, J. H. *Adv. Mater.* **1996**, *8*, 637.
(28) Kotov, N. A.; Haraszti, T.; Turi, L.; Zavala, G.; Geer, R. E.; Dekany, I.; Fendler, J. H. *J. Am. Chem. Soc.* **1997**, *119*, 6821.
(29) Cassagneau, T.; Fendler, J. H. *Adv. Mater.* **1998**, *10*, 877.
(30) Kovtyukhova, N.; Buzaneva, E.; Senkevichi, A. *Carbon* **1998**, *36*, 549.

10.1021/cm990043i CCC: $18.00
Published on Web 05/15/1999

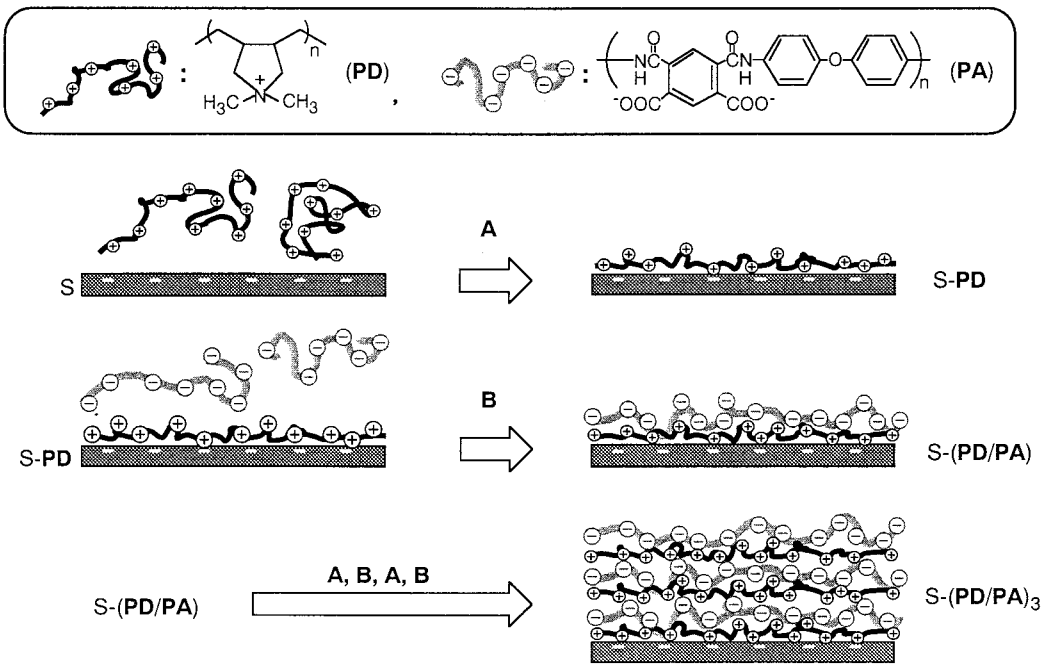

Figure 1. Schematics of the layer-by-layer self-assembly of **PD** and **PA** on a sbustrate (S): (A) adsorption of **PD** and (B) adsorption of **PA**.

Experimental Section

Materials. Poly(diallyldimethylammonium chloride), **PD**, (20 wt % aqueous solution) was obtained from Aldrich Chemical Co. and all of the other chemicals (hydrochloric acid, sodium hydroxide, sulfuric acid, hydrogen peroxide, toluene) were reagent grade (J. T. Baker, Inc.). Water was purified by using a Millipore Milli-Q filter system provided with a 0.22 μm Millistack filter at the outlet.

Poly(amic acid), **PA**, was synthesized from pyromellitic dianhydride (PMDA, Tokyo Kasei Co.) and 4,4′-oxydianiline (ODA, Tokyo Kasei Co.) according to the procedure previously reported.[31,32] Briefly, an equimolecular amount of ODA (3.0 g) was added dropwise into a *N*,*N*-dimethylacetamide (DMAc, Tokyo Kasei Co., 50 mL) solution of PMDA (3.27 g) with stirring under a stream of N_2 gas at 15 °C. After further stirring for 1 h at 15 °C and for 3 h at 25 °C, the viscous liquid was precipitated by pouring it into ethanol (1500 mL) and purified by repeating the reprecipitation by pouring the DMAc solution (50 mL) into ethanol (1500 mL) three times (yield 90%).

Self-Assembly of (PD/PA)$_n$ Films. Quartz and mica were used as substrates, S, for the self-assembly. The surface of quartz was cleaned by immersion into a H_2SO_4:H_2O_2 = 7:3 (v/v) solution for a few minutes followed by washing with copious amounts of Milli-Q water and drying with N_2 gas stream. Mica was freshly cleaved with an adhesive tape just prior to use.

Self-assembly of an ultrathin film of one sandwich layer on a substrate, containing a nanolayer of **PD** and a nanolayer of **PA**, S−(**PD**/**PA**), involved the following steps: (i) immersion of S into a 10 mM aqueous **PD** solution, kept at pH = 9 (no buffer),[33] for 5 min; (ii) rinsing for 10 s with a dilute aqueous NaOH solution (pH 9); (iii) immersion into a 10 mM aqueous **PA** solution, kept at pH = 9, for 5 min; (iv) washing with a dilute aqueous NaOH solution (pH 9). Each washing was followed by drying in a stream of N_2 gas for 30 s. A subsequent *n* number of sandwich layers, to produce an ultrathin film containing alternating *n* layers of **PD** and *n* layers of **PA**, S−(**PD**/**PA**)$_n$, were prepared by repeating steps i−iv *n* times as shown in Figure 1.

The self-assembly was monitored by means of ultraviolet−visible (UV−vis) spectrophotometry and by using a quartz crystal microbalance. UV−vis absorption spectra of the quartz-supported films were recorded on a diode array spectrometer (Hewlett-Packard Model 8452A). QCM measurements were carried out in air at room temperature (25 °C) using a Sogo Pharmaceutical Co. SF-105A microbalance with a 9 MHz AT-cut quartz resonator. Prior to the self-assembly, the surface of evaporated gold (on quartz resonator) was derivatized by immersing it into 0.1 M ethanolic solution of 2-amino-1-ethanethiol (AET, Tokyo Kasei Co.) for 60 min. The AET-derivatized resonator was then used as a substrate for the self-assembly of **PA** and **PD** under the same condition as described above. Frequency shifts of each layer (after drying in a stream of N_2) was determined and converted to mass increase by means of the Sauerbrey equation.[34] A frequency decrease of 1 Hz corresponded to a mass increase of 0.9 ng in the present system.

PD/**PA** complex powders were also prepared by mixing 10 mM aqueous **PA** solution with 10 mM aqueous **PD** solution at the molar ratio of polymer unit **PA**:**PD** = 1:2. The **PD**/**PA** complex was obtained by centrifugation followed by drying for 1 day under a reduced pressure in a desiccator. The composition of the **PD**/**PA** complex was determined by elemental analysis (C 49.60%, H 8.10%, 6.10%, for $(PD)_{2.3}(PA)\cdot 8H_2O$).

Conversion of S−(PD/PA)$_n$ Films into Carbon Nanofilms. Heating the S−(**PD**/**PA**)$_n$ films to 1000 °C at a rate of 15 °C min^{-1} under a stream of N_2 and keeping them at 1000 °C for 5 min in a furnace (Lindverg Bleum Co., Model STF55433C) resulted in the formation of carbon films. To confirm the formation of polyimide as an intermediate, the S−(**PD**/**PA**)$_n$ films were heated only to 300 °C and were immediately taken out of the furnace and characterized by absorption spectrophotometry.

The S−(**PD**/**PA**)$_n$ films heated to 1000 °C were characterized by elementary analysis, X-ray diffraction (XRD), and electric

(31) Sroog, C. E. *Macromolecular Synthesis*; Moore, J. A., Ed.; John Wiley & Sons: NewYork, 1977; Collect. Vol. 1, p 295.
(32) Nishikata, Y.; Kakimoto, M.; Morikawa, A.; Imai, Y. *Thin Solid Films* **1988**, *160*, 15.
(33) To maintain the ionized form of **PA**, the pH of the washing solutions was adjusted to 9.00.
(34) Sauerbrey, G. *Z. Phys.* **1959**, *155*, 206.

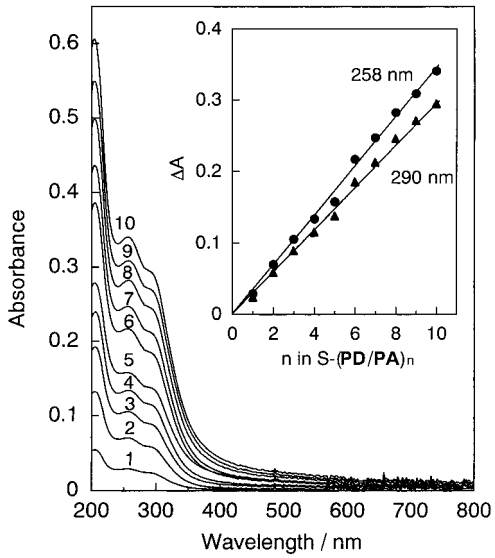

Figure 2. UV−vis spectra of self-assembled S−(**PD**/**PA**)$_n$ films with $n = 1-10$. The inset shows plots of absorbances at 258 and 290 nm against n.

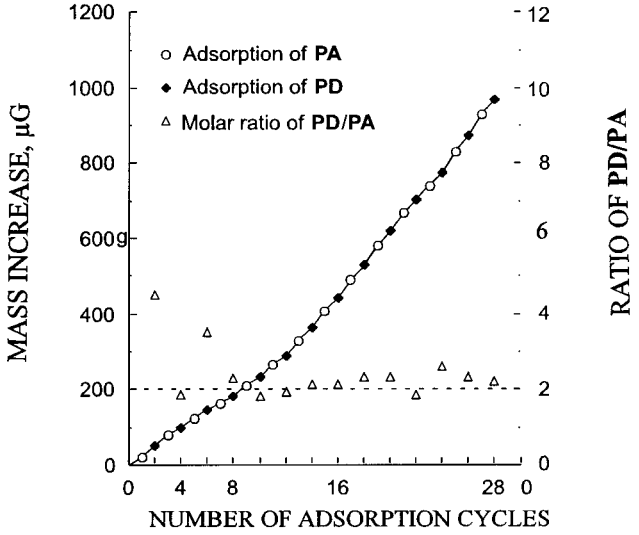

Figure 3. Increases of mass and molar ratio of **PD**/**PA** as a function of the number of deposition cycles, determined by QCM. The dotted line indicates the stoichiometric molar ratio of polymer units corresponding to charge balance between **PA** and **PD** (i.e., **PA**/**PD** = 2.0).

resistance measurements. XRD measurements were carried out by using a Siemens Co. (Kristalloflex K-710) diffractometer with Cu Kα radiation. Electrical resistances of the pyrolyzed S−(**PD**/**PA**)$_n$ films were measured, in air, by a two-electrode system by using electromultimeter (Fluke 85). Two 5-mm-long electrodes, separated from each other by a distance of ∼3 mm were attached to the surface of the self-assembled films by silver paste (Electron Microscopy Sciences Co.). Connections to the electrometer were made by copper wires, also attached to the two-electrodes by silver paste. Resistivities, R_s (R_s is the resistance of a centimeter cube of a substance to passage of an electric current perpendicular to two parallel faces, which can be expressed by $R_s = R(A/L)$, where R is measured resistance, $A = dr$, d = thickness of the self-assembled films, r = length of the electrodes, and L is the distance of between two electrodes) were converted to sheet resistivity (R_{sq}), using the relationship: $R_{sq} = R_s/d = R(r/L)$.

The pyrolysis of **PD**/**PA** complex powder was also examined by means of thermogravimetry (TG) under a stream of N_2 gas at a heating rate of 15 °C min^{-1} (Seiko Instruments Inc. TG-DTA 200) and IR spectrophotometry (Perkin-Elmer 1650).

Other Instrumental Analysis. Atomic force microscopy (AFM) and scanning tunneling microscopy (STM) were performed by using a Topometrix Explorer 2000 scanning probe microscope. AFM images of mica- and quartz-supported films were taken in air in the noncontact mode with a 2 μm scanner and silicon nitride tips (spring constant = 34−44 N m^{-1}, F_o = 176 kHz). STM images of quartz-supported carbon films were acquired in constant-current mode (5 mA) with a tungsten-wire tip (0.01−0.1 V tip bias). These images were examined at least at three different sites in a given sample. Thickness of the carbon film (formed on the half-side of quartz plate) was evaluated by incident angle dependent reflectivity measurement as the same manner already reported.[26,35]

Results and Discussion

Self-Assembly of S−(PD/PA)$_n$ Films. Ultrathin films of poly(amic acid), **PA**, and poly(diallyldimethylammonium chloride), **PD**, were layer-by-layer self-assembled on different substrates. Quartz-supported S−(**PD**/**PA**)$_n$ films exhibited absorption peaks at 205, 258, and 290 nm (Figure 2).[36] Monitoring these absorbances as a function of substrate immersion times established 5-min dipping as optimal for the adsorption of **PD** and **PA** electrolytes. Absorbances at 205, 258, and 290 nm of quartz-supported S−(**PD**/**PA**)$_n$ films increased linearly with increasing n (see the inset of Figure 2). No difference in the absorption spectra was observed for S−(**PD**/**PA**)$_n$ films on quartz ($n = 1-30$) prior to and after the adsorption of additional **PD** layer. These results substantiate the regular adsorption of **PD** and **PA** in the self-assembly and reproducibility of the S−(**PD**/**PA**)$_n$ films formed.

The mass of a layer of **PA** (or **PD)** adsorbed during the self-assembly was also examined by QCM measurement using a 2-amino-1-ethanethiol (AET) derivatized resonators as substrates. Although the mass increase was continuous with increasing n in the S−(**PD**/**PA**)$_n$ films the slope in the plot of mass deposited vs the number of times **PD** and **PA** deposited changed at $n = 5$ (Figure 3). The mass of each **PD** layer adsorbed was observed to be in the range of 14−28 ng for $n = 1-5$ and 29−41 ng for $n > 5$. Similarly, The mass of each **PA** layer adsorbed was observed to be in the range of 21−30 ng for $n = 1-5$ and 42−59 ng for $n > 5$.

Taking into account the adsorbing area of the resonator (0.336 cm^2) and the specific gravities of **PD** and **PA** bulk polymers (1.24 and 1.4 g/cm^3),[37] permitted the assessment of the thickness of an adsorbed layer. The thickness of a **PD** layer was estimated to be 0.45 ± 0.15 nm prior and 0.8 ± 0.2 nm after the fifth deposition

(35) Zhao, X. K.; Xu, S.; Fendler, J. H. *J. Phys. Chem.* **1994**, *98*, 8827.

(36) Kakimoto, M.; Suzuki, M.; Konishi, T.; Imai, Y.; Iwamoto, M.; Hino, T. *Chem. Lett.* **1986**, 823.

(37) Specific gravity of **PD** was calculated to be 1.24 using the Aldrich catalog value (published in 1997) of 20% aqueous **PD** solution (1.04). The specific gravity of **PA** is unavailable, and the Aldrich catalog value (published in 1997) of poly[*N*,*N*′-(1,4-phenylene)-3,3,4,4′-benzophenonetetracarboxylic amic acid] (1.40) was used for reference. Each layer thickness was calculated by using the equation of $t = m/(rA)$; where t is thickness, m is mass increase, r is specific gravity, and A is adsorbing area on resonator (0.336 cm^{-3}).

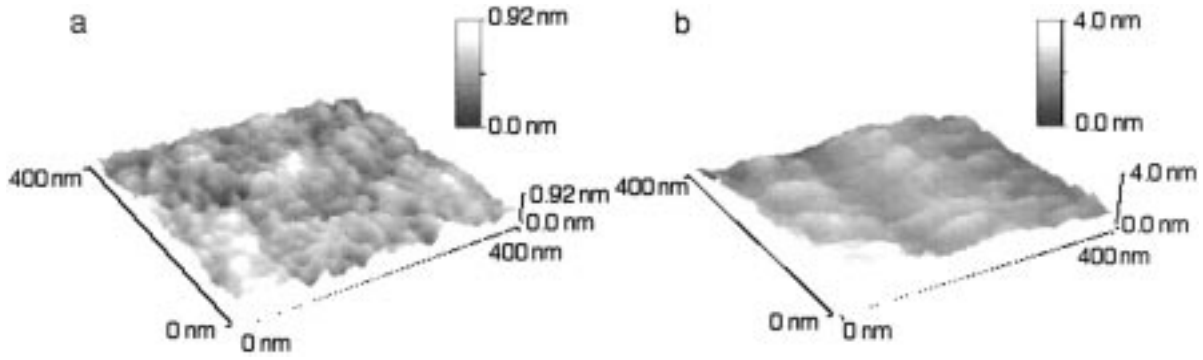

Figure 4. AFM images of surfaces of S-**PD** film and of self-assembled S−(**PD**/**PA**)$_1$ film on mica substrate.

cycle. Similarly, the thickness of a **PA** layer was estimated to be 0.60 ± 0.15 nm prior and 1.2 ± 0.2 nm after the fifth deposition cycle. Apparently, deposition of less than five sandwich layers resulted in incomplete and/or uneven substrate coverage. This is most likely to originate in the incomplete protonation of the amino groups at the AET surface at pH = 9.0 The molar ratio of **PD** to **PA** in the same deposition cycle was close to 2 at above n = 5 (see Figure 3), indicating an almost stoichiometric adsorptions.

The topography of mica-supported S−(**PD**/**PA**)$_n$ films was investigated by AFM. The first layer of **PD** (S−**PD**) showed a featureless AFM image with a height variation of about 1 nm (Figure 4a), consistent with films that have been reported previously.[16] Adsorption of a layer of **PA** onto the S−**PD** film manifested itself in the formation of a relatively rough surface with height variation of around 4 nm (Figure 4b). Self-assembly of the second layer of **PD** to form the S−(**PD**/**PA**)/**PD** film decreased the height variation to below 3 nm. Similar images were obtained repeatedly with the subsequent alternating adsorption of **PA** and **PD**. These observations support the schematics in Figure 1 for the self-assembly of S−(**PD**/**PA**)$_n$ films.

Conversion of S−(PD/PA)$_n$ Films into Carbon Nanofilms. The thermal gravimetric (TG) curves of **PD**, **PA**, and mixed **PD** and **PA** powders under a stream of N_2 gas are shown in Figure 5. **PD** thermally decomposed from 300 °C to 480 °C (Figure 5a), and **PA** showed a two-step weight loss until 1000 °C (Figure 5b). The first weight loss of **PA** up to 300 °C was due to release of adsorbed solvent and dehydration with conversion into the polyimide, which was confirmed by concomitant appearance of IR absorption bands at 1780, 1730, and 1380 cm^{-1}, due to the imide groups.[36,38] The second weight loss of **PA** above 530 °C was consistent with the previously reported TG curve of polyimide in which the weight loss due to carbonization started at around 500 °C and its value was 40.7% at 1000 °C.[39] The mixed **PD** and **PA** powder showed a TG curve composed of the combined weight losses of **PD** and **PA** (Figure 5c) and the formation of polyimide structure in the complex was confirmed by the IR measurement. Heating the mixed **PD** and **PA** powders to 1000 °C resulted in 80% weight loss, which was consistent with the value based on the

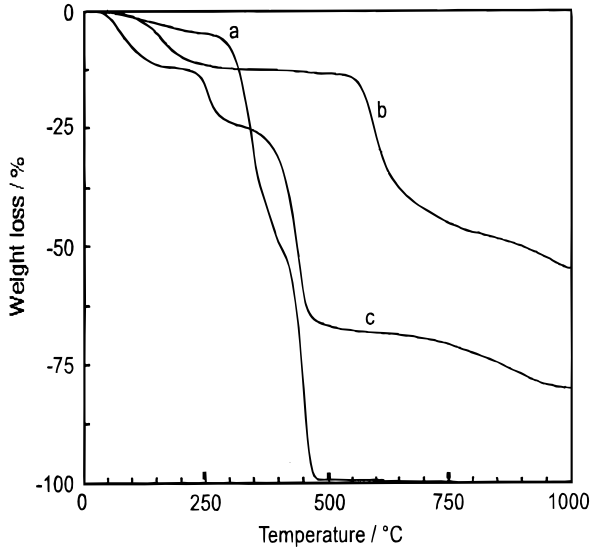

Figure 5. TG curves of **PD** (a), **PA** (b), and **PD**/**PA** complex (c) under a stream of N_2 gas.

elemental analysis (**PD**$_{2.3}$**PA**·8H_2O, 78%). The composition of the pyrolyzed mixture of **PD** and **PA** powder heated to 1000 °C was determined by elementary analysis to be C 80.55%, H 2.48%, and H 1.43%, giving atomic ratios of C/N = 56.33 and C/H = 32.48 (as compared to the unheated mixture of **PD** and **PA** powder: C 49.60%, H 8.10%, and N 6.10%; giving atomic ratios of C/N = 8.13 and C/H = 6.12%). The increase in the atomic ratios of C/N and C/H upon heating the self-assembled films to 1000 °C substantiates the formation of a carbonaceous, graphite-like material in the pyrolysis (Figure 6).

The film obtained by heating S−(**PD**/**PA**)$_n$ to 300 °C showed UV−vis absorptions bands at 220 and 280 nm, characteristic of polyimide[35] (Figure 7b). The UV−vis absorbances of these films increased proportionally with the increase of n in S−(**PD**/**PA**)$_n$, indicating the regularity of polyimide formation. Further heating to 1000 °C, resulted in the disappearance of the absorption peaks at 220 and 280 nm and in the concomitant appearance of a new broad absorption with a maximum at 276 nm (Figure 7c). A similar broad absorption (centered at 280 nm), observed in the pyrolysis of Langmuir−Blodgett films, prepared from aromatic polymers, was attributed to the formation of graphite-like carbonaceous material.[11] A linear relationship was obtained for the pyrolyzed film between the absorbance at 276 nm and n of

(38) Jeon, N. L.; Nuzzo, R. G. *Langmuir* **1995**, *11*, 341.
(39) Inagaki, M.; Ibuki, T.; Takeichi, T. *J. Appl. Polym. Sci.* **1992**, *44*, 521.

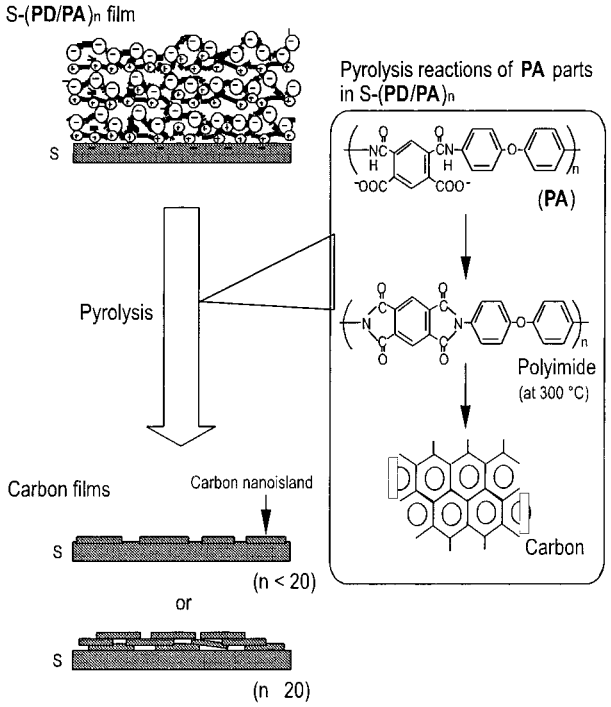

Figure 6. Schematics of the formation of carbon nanofilms from the S−(**PD**/**PA**)$_n$ films.

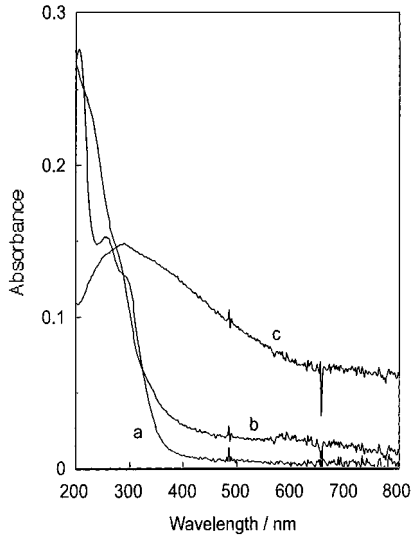

Figure 7. UV−vis spectra of S−(**PD**/**PA**)$_5$ film before (a) and after heat treatments (b, heating to 300 °C and, c, heating to 1000 °C).

(**PA**/**PD**)$_n$ film. The XRD patterns of the pyrolyzed S−(**PD**/**PA**)$_{20}$ film heated to 1000 °C showed two broad peaks at 2θ of 15−35° and 40−50° (Figure 8). Although the peak broadening implies a disordered structure, these peaks are assignable to diffraction originating in the (002) and (100) or (101) planes of natural graphite (2θ = 26.5°, 42.4°, 44.6°, respectively).[10] These results can be taken to imply the formation of graphite-like carbon films in the pyrolysis of S−(**PD**/**PA**)$_n$.

Characterization of Pyrolytic Carbon Nanofilms. The sheet resistivity per (**PD**/**PA**) unit layer was found to decrease with the increase of n in (**PD**/**PA**)$_n$ film until n = 20 after which it leveled off (Figure 9). The conductivity of the pyrolyzed films at $n \geq 20$ was calculated to be 150−200 S cm^{-1}

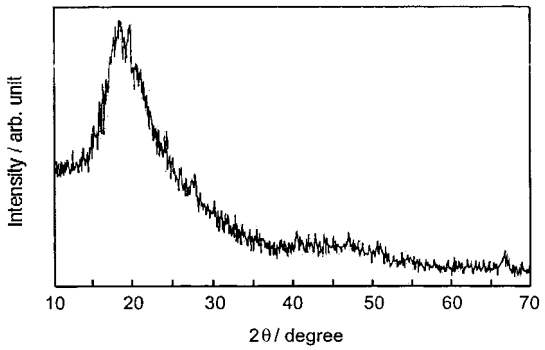

Figure 8. XRD pattern of pyrolyzed S−(**PD**/**PA**)$_{20}$ film heated to 1000 °C and held at 1000 °C for 5 min.

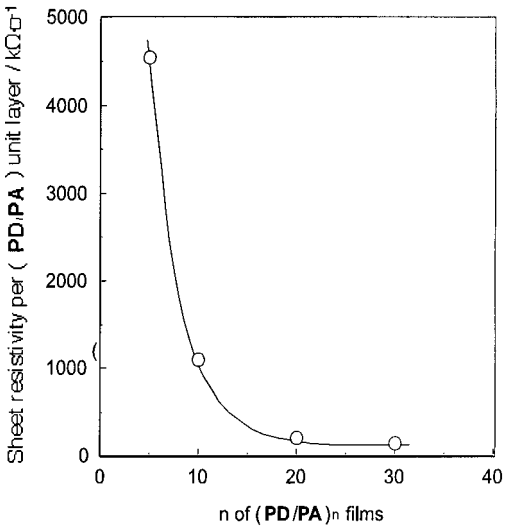

Figure 9. Relationship between sheet resistivity of carbon films per (**PD**/**PA**) unit layer and n of S−(**PD**/**PA**)$_n$ precursor films.

by using a thickness determined by incident angle dependent reflectivity measurement (8.2 ± 0.2 nm for n = 20, 14.5 ± 0.2 nm for n = 30; average thickness d/n = 0.4−0.5 nm). The value of conductivity is comparable to those reported for bulk pyrolyzed polyimide (160 S cm^{-1} for samples heated in a vacuum,[8] 100 S cm^{-1} for samples heated in the flow of N_2 gas[37] for 1 h) and to that obtained for Langmuir−Blodgett films (300 S cm^{-1} for samples heated for 1 h in the flow of N_2 gas),[11] indicating that pyrolysis of the S−(**PD**/**PA**)$_n$ films produces highly conductive carbonaceous films.

Topographies of pyrolyzed S−(**PD**/**PA**)$_n$ films were investigated by AFM and STM. A number of isolated 400-nm-diameter laminar islands with a height of around 10 nm were observable in pyrolyzed S−(**PD**/**PA**)$_5$ films by AFM (Figure 10a). Increasing n, by depositing additional layers of **PD** and **PA** increased the densities of domains (see, for example, the image of a pyrolyzed S−(**PD**/**PA**)$_{20}$ films in Figure 10b), until the film became contiguous. Increase of electrical conductivity with increasing n in pyrolyzed S−(**PD**/**PA**)$_n$ films is the consequence of formation of connected carbonaceous films as proposed in Figure 6. Nevertheless, STM images indicated the presence of a large number of defects, on the surface of laminar carbon nano islands.

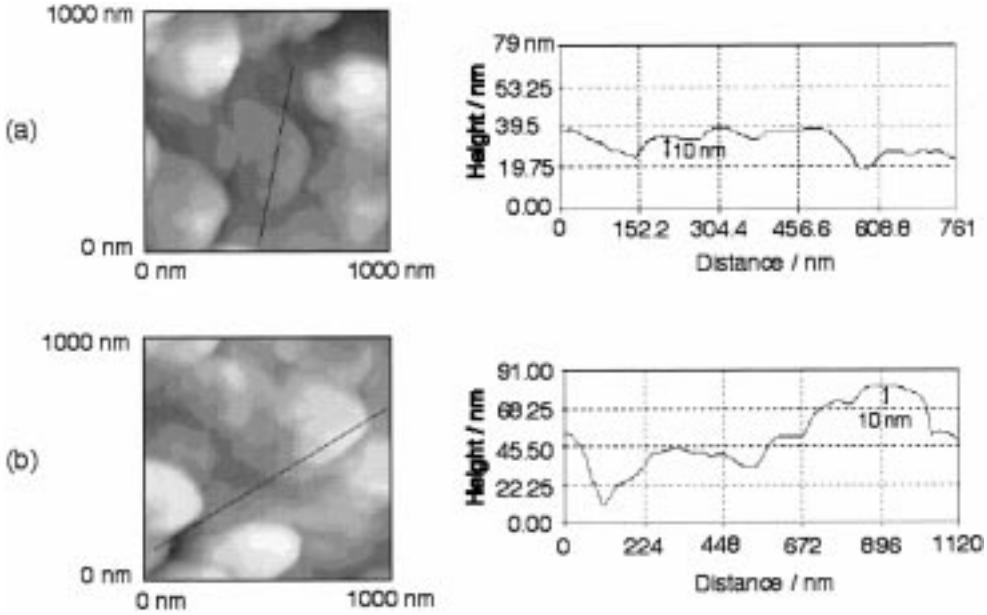

Figure 10. AFM images of pyrolytic carbon films prepared from S−(**PD**/**PA**)$_5$ film (a) and S−(**PD**/**PA**)$_{20}$ film (b).

Conclusion

Fabrication of graphite-like carbonaceous ultrathin films, with conductivities in the 150−200 S cm^{-1} range, by the pyrolysis of layer-by-layer self-assembled nanometer-thick oppositely charged polyelectrolytes is the most significant accomplishment of the present work. Judicious manipulations of the types of polyelectrolytes employed and the heating conditions will lead, we are confident, to defect-free films with even higher conductivities.

Acknowledgment. This study was supported by The Foundation of Kyushu Industrial Technology Center in Japan.

CM990043I